OPEN ACCESS

Deterministic entanglement and tomography of ion–spin qubits

New Journal of Physics
The open–access journal for physics

Deterministic entanglement and tomography of ion–spin qubits

J P Home, M J McDonnell, D M Lucas, G Imreh, B C Keitch, D J Szwer, N R Thomas, S C Webster, D N Stacey and A M Steane[1]

Centre for Quantum Computation, Clarendon Laboratory, Department of Physics, University of Oxford, Parks Road, Oxford OX1 3PU, UK
E-mail: a.steane1@physics.ox.ac.uk

New Journal of Physics **8** (2006) 188
Received 7 June 2006
Published 12 September 2006
Online at http://www.njp.org/
doi:10.1088/1367-2630/8/9/188

Abstract. We have implemented a universal quantum logic gate between qubits stored in the spin state of a pair of trapped ^{40}Ca ions. An initial product state was driven to a maximally entangled state deterministically, with 83% fidelity. We present a general approach to quantum state tomography which achieves good robustness to experimental noise and drift, and use it to measure the spin state of the ions. We find the entanglement of formation is 0.54.

In recent years, entanglement has been detected and used in a variety of physical systems, but the number in which it can be created under deterministic control with good fidelity remains small. We present the implementation of a universal two-qubit quantum logic gate in a trapped ion experiment, demonstrating deterministic entanglement with 83% fidelity. Tomography was performed using a method robust against noise sources of practical relevance in the experiments. Our results illustrate the relative insensitivity of the gate to the initial temperature of the ions.

The logic gate exploits the oscillating force method [1]–[5]. Our study differs from previous trapped-ion experiments in the physical nature of the qubit, the trapping parameters, the light fields used to implement logic at the ions, and the laser sources, as follows.

First, each qubit is stored in a pure spin-half system, the spin of a ^{40}Ca ion in its ground state. Previous studies used hyperfine structure [1], [6]–[8] or a pair of electron orbitals [9, 10].[2] The spin-half system is convenient in its simplicity. The absence of 'spectator levels', i.e. other states nearby in energy, reduces the movement of population out of the controlled Hilbert space.

[1] Author to whom any correspondence should be addressed.
[2] Ion–spin qubits are entangled in H Häffner *et al* (2005 *Appl. Phys.* B **81** 151), by transfer from an $S_{1/2}/D_{5/2}$ qubit.

PII: S1367-2630(06)26327-4

This process, sometimes called leakage error, is not directly correctable by quantum error correction [11, 12]. Spectator levels also exacerbate decoherence by photon scattering during the gate operation.

Next, our trap is comparatively large [13], so electric field noise from fluctuating patch potentials and Johnson noise in the electrodes is very small [14, 15]. We have measured very low heating rates, of order a few phonons per second, in the trap.

We use a single laser field to apply all the operations (single ion rotations and the two-qubit gate), changing only the amplitude and frequency to switch from one operation to another. This reduces the experimental complexity, and opens the possibility of future work in which the different parts of a pulse sequence could be brought together in a single chirped and shaped pulse.

Finally, the laser sources in our apparatus are all small semiconductor diodes, which do not require frequency doubling and which could in principle be packaged on a small optical chip. We thus begin to address the optical part of the challenge to scale this type of system up to a powerful quantum computer [16]–[18].

Let the spin-up/down states $|\uparrow\rangle, |\downarrow\rangle$ be the computational basis states of a qubit. We implement the two-qubit controlled-phase gate $Z_1(\phi_1)Z_2(\phi_1)G(\Psi)$ where $Z_k(\phi_1)$ is a rotation of qubit $k = 1, 2$ by ϕ_1 about the quantization axis, and $G(\Psi)$ is a two-qubit operator represented in the computational basis $|\uparrow\uparrow\rangle, |\uparrow\downarrow\rangle, |\downarrow\uparrow\rangle, |\downarrow\downarrow\rangle$ by the diagonal matrix $\mathrm{diag}(1, \exp(\mathrm{i}\Psi), \exp(\mathrm{i}\Psi), 1)$. For $\Psi = \pi/2$, or an odd multiple of $\pi/2$, this is equivalent to controlled-not up to single qubit rotations.

The gate mechanism is described in [1]. A spin-dependent force oscillating at frequency ω is applied to the pair of ions. Let $f_k(m)$ be the complex amplitude of the force on ion k when it is in spin state $m = \uparrow, \downarrow$. The COM (stretch) mode is excited by the sum (difference) force $f_1(m_1) \pm f_2(m_2)$ respectively. The effect on the quantum harmonic motion is simply to displace the state in its z–p phase space (as long as the position-dependence of the force is negligible during the displacement [19]). By choosing ω close to one of the normal mode frequencies, one can enhance the displacement and also simplify the dynamics, because then the excited mode simply describes a circle in phase space, which closes after time $2\pi/\delta$, and the excitation of the other mode can be neglected. This motion causes the system to acquire a phase ϕ_L proportional to the area of the loop in phase space.

Many arrangements are possible. We adopt $f_1(m) = f_2(m)$, then the stretch mode is excited only for anti-aligned spin states. By tuning close to the stretch mode frequency ω_s, i.e. $|\delta| \ll \omega_\mathrm{s} - \omega_\mathrm{c}$ where $\delta \equiv \omega - \omega_\mathrm{s}$ and ω_c is the COM mode frequency, we then have $\Psi = \phi_\mathrm{L} = (\pi/2)(\Omega_\mathrm{f}/\delta)^2$ where $\Omega_\mathrm{f} = |f(\uparrow) - f(\downarrow)|z_{0\mathrm{s}}/\hbar$, $z_{0\mathrm{s}} = (\hbar/(4M\omega_\mathrm{s}))^{1/2}$ and M is the mass of one ion.[3]

To measure the spin state of the ion pairs, we developed the following quantum state tomography method. Tomography in general requires the accumulation of a sufficient set $\{M_i\}$ of measurements of a given state ρ (many copies of which are needed), in order to allow ρ to be reconstructed to some desired accuracy from $\{M_i\}$. Usually rotations are applied to the system which is then measured in a fixed basis.

This problem has been studied in various settings and, for example, sets of $\{M_i\}$ of minimal size, or designed for certain experimental situations, have been discovered [20]. Our method is

[3] The motion leads to a two-qubit effect, $\Psi \neq 0$, only if $\omega_\mathrm{s} \neq \omega_\mathrm{c}$. Since this difference is owing to the ions' Coulomb repulsion, the two-qubit gate relies, as expected, on a two-body interaction.

designed to be robust against noise and drift problems, and to be convenient in a fairly broad range of experimental settings. We achieve this by a judicious choice of rotation angles and by accumulating data sets in a form that should be well fitted by sums of orthogonal sinusoidal functions of known period. The least squares fit is robust because the functions in the fit are orthogonal, it averages the data over many timescales, and many noise processes affect the residuals not the fitted parameter values.

Let $R(\theta, \phi)$ be a rotation of a single qubit through θ on the Bloch sphere about an axis of azimuthal angle ϕ. To analyse a given density matrix ρ, the qubits are first rotated and then measured in the $|\uparrow\rangle, |\downarrow\rangle$ basis, then ρ is re-prepared and one repeats with either the same or new rotation angles, until a sufficient set $\{M_i\}$ has been acquired. Experimentally θ depends on a pulse area, ϕ on the phase of an r.f. oscillator. The latter is more easily adjusted than the former to a variety of precisely known values. Therefore we only use two values of θ, but many values of ϕ, see figure 3. For clarity, we give details for the case of two-qubits both undergoing the same rotation, but the principles apply more generally. In this restricted case, a general ρ can be almost, but not fully reconstructed.

Write $\rho = \sum_{i,j=0}^{3} c_{ij}\hat{\sigma}_i \otimes \hat{\sigma}_j$ where $\hat{\sigma}_i$ are the Pauli spin operators (starting with $\hat{\sigma}_0 = I$ the identity). Let $P(m_1, m_2)$ be the populations of ρ and $P_{\mathrm{R}}(m_1, m_2)$ be the populations after the rotation $R(\theta, \phi)$ has been applied to both qubits. Then

$$P_{\mathrm{R}}(\uparrow\uparrow) = a_{\uparrow\uparrow} + b_{\uparrow\uparrow}\cos(\phi) + c_{\uparrow\uparrow}\sin(\phi) + d_{\uparrow\uparrow}\cos(2\phi) + e_{\uparrow\uparrow}\sin(2\phi) \tag{1}$$

and similarly for $\uparrow\downarrow, \downarrow\uparrow$, where the coefficients a–e are simple sinusoidal functions of θ. By choosing different values of θ and ϕ, 12 independent real numbers can be extracted from the population measurement outcomes. Therefore three of the 15 independent real numbers which fully characterize ρ are not available when both qubits undergo the same rotation.

The tomography method consists of accumulating data at given θ as a function of ϕ, then fitting equation (1) and its partners for $P_{\mathrm{R}}(\uparrow\downarrow)$, $P_{\mathrm{R}}(\downarrow\uparrow)$ to the data, with the a–e coefficients as fitted parameters, cf figure 3. After using two θ values, the density matrix coefficients c_{ij} can be found from θ and a–e (with some redundancy). The inferred matrix ρ^{M} is not guaranteed to be positive definite. One can handle this by any suitable approach, for example by searching among physical density matrices ρ^{P} for the one which most closely matches ρ^{M} by some measure. We adopt this 'maximum likelihood' method using the cost function $\sum_{i,j} |\rho^{\mathrm{P}} - \rho^{\mathrm{M}}|^2_{ij}$ where ρ^{P} is positive definite [21].

The apparatus consists of a linear r.f. Paul trap and laser system largely as described in [13]. We load single or pairs of ^{40}Ca ions by photoionization. A 6.3 MHz r.f. field provides radial confinement, with radial COM frequency $\simeq$1 MHz. Axial confinement is provided by dc endcaps, tuned as described below. 397 and 866 nm lasers are used for Doppler cooling, fluorescence detection and spin state preparation (with 99% fidelity) by optical pumping. A further pair of lasers performs spin-state-selective shelving to $D_{5/2}$, which allows the fluorescence to be used to read out the spin state (with $\sim$90% fidelity), see [22]. The ions are cooled in three dimensions by Doppler cooling, and along z by Raman sideband cooling to $\bar{n}_{\mathrm{com,str}} \simeq 0.2,\ 0.2$, measured as in [23].

The light field used for pulsed sideband cooling and all the coherent operations is a walking wave created by laser beams A, B (shown in figure 1) propagating at $\theta_{\mathrm{L}} = 58.9^\circ$ to each other, with difference wavevector $\Delta k = 4\pi \sin(\theta_{\mathrm{L}}/2)/\lambda$ directed along the trap axis z. A quantization axis is set by a weak magnetic field directed at 3° to beam B (and $\theta_{\mathrm{A}} = 62^\circ$ to beam A).

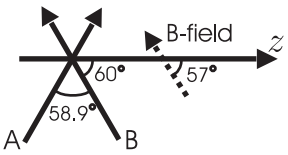

Figure 1. The directions of the laser beams A and B used for coherent operations, relative to the trap axis z. The magnetic field direction is also shown (dashed line).

All these axes are horizontal. To reduce sensitivity to the pulse area, we balance the ac Stark shifts on $|\uparrow\rangle$, $|\downarrow\rangle$ from either beam acting alone, using Ramsey interferometry. This results in polarization very close to linear,[4] which we make at angle β to the vertical for A, and horizontal for B. Each beam illuminates both ions equally. They are derived from the same laser, at a frequency detuned $\Delta_L/2\pi = 30$ GHz above the $S_{1/2} - P_{1/2}$ transition. A precise frequency difference $\omega = \omega_A - \omega_B$ is introduced between them by acousto-optic modulation.

The Zeeman splitting of $|\uparrow\rangle$ from $|\downarrow\rangle$ is $\omega_0 = 2\pi \times 4800$ kHz. At $\omega = \omega_0$ spin-flip transitions are resonantly driven by the π component of A combined with the σ^- component of B. Let Ω_c be the Rabi frequency for this 'carrier' Raman process. The oscillating force is created by the periodic light shift from the $\sigma^{\pm}$ components of the walking wave. The coupling strength Ω_s is given by $\Omega_s = \sqrt{2}\Omega_c\epsilon_+/\epsilon_\pi$, where ϵ_+, ϵ_π are polarization amplitudes for beam A. For our geometry, $\sqrt{2}\epsilon_+/\epsilon_\pi = \cot\theta_A/\cos(\Delta\phi/2)$ and $\Omega_f = 2\eta\Omega_s \sin(\Delta\phi/2)$, where $\eta = \Delta k z_{0s}$ is the stretch mode Lamb–Dicke parameter, and $\Delta\phi$ is the phase angle between the forces, given by $\tan(\Delta\phi/2) = (\cos\theta_A \tan\beta)^{-1}$.

During the force pulse at $\omega \simeq \omega_s$, the carrier process is driven off-resonantly at detuning $\omega_0 \pm \omega$. For $\omega_0 \pm \omega \gg \Omega_c$, the qubit states are pushed apart by a light shift

$$\Delta_c = \frac{\Omega_c^2}{2}\left[\frac{1}{\omega_0 + \omega} + \frac{1}{\omega_0 - \omega}\right]. \tag{2}$$

This is of the order 4 kHz in our experiments, and it gives rise to the single-qubit rotations $Z_k(\phi_1)$ in the gate, with $\phi_1 = \Delta_c\tau$.

To achieve $f_1(m) = f_2(m)$, we adjust ω_c so that the ions' separation $d \simeq 9\,\mu$m is an integer number p of standing wave periods, $\Delta k d = 2\pi p$. We used $p = 22$, $\omega_c/2\pi = 500$ kHz ($\eta = 0.133$) in one experiment, and $p = 21$, $\omega_c/2\pi = 536.5$ kHz ($\eta = 0.128$) in another.

A given experimental sequence consists of cooling, spin preparation in $|\downarrow\downarrow\rangle$, then a spin echo sequence with the force pulse $\mathcal{W}$ of duration τ in one or both of the gaps, followed by an analysis pulse and then spin state measurement; see inset to figure 2(b). The analysis pulse is the rotation $R(\theta, \phi)$ in the tomography scheme. A perfect implementation would produce the maximally entangled state

$$|E(r)\rangle \equiv (|\uparrow\uparrow\rangle + e^{ir}|\downarrow\downarrow\rangle)/\sqrt{2} \tag{3}$$

before the analysis pulse, with $r = 2\phi_1 - \pi/2$. To assess the state ρ obtained in practice we use the fidelity $F \equiv \max_r\langle E(r)|\rho|E(r)\rangle$. This compares ρ with the most closely matching member of the class $|E(r)\rangle$.[5]

[4] Beam A drives the carrier by a Raman process off-resonant by the Zeeman splitting of $|\uparrow\rangle$ and $|\downarrow\rangle$. This creates a light shift whose cancellation results in $\epsilon_-/\epsilon_+ \simeq 1.02$ for this beam.

[5] This choice is reasonable because it is equivalent to using the data to extract the value of r.

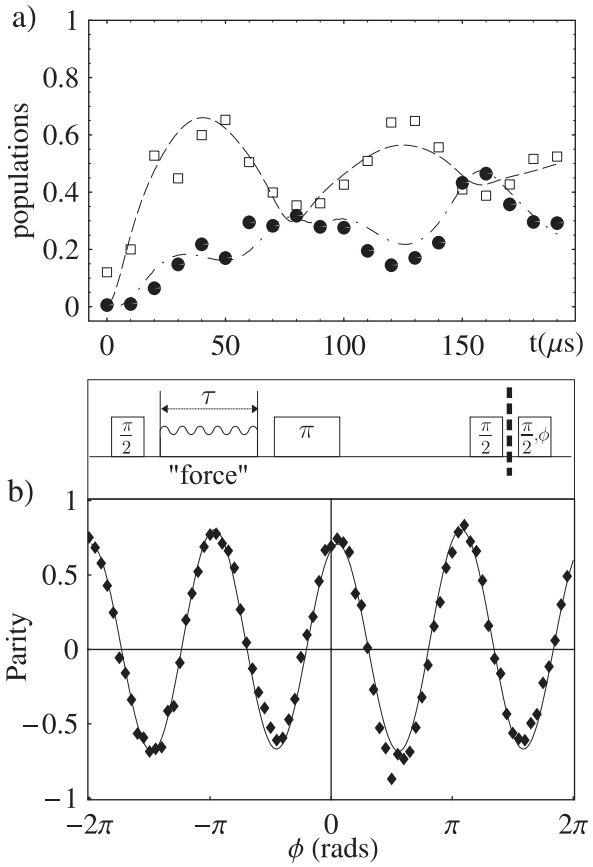

Figure 2. (a) Measured populations $P(\uparrow\uparrow)$, $P(\uparrow\downarrow) + P(\downarrow\uparrow)$ (●, □) versus τ after a spin-echo sequence with $\mathcal{W}(\tau)$ in the first gap, at $\delta/2\pi = 12.6\,\text{kHz}$. Each point is the average of 500 repeats of the experimental sequence. The lines are fitted curves, using a model which assumes each qubit decoheres independently at rate Γ. (b) Parity signal vs. ϕ after a $\theta = 0.46\pi$ analysis pulse, for $\tau = 77\,\mu\text{s}$. Each point is the average of 1000 repeats of the experimental sequence. The inset shows the pulse sequence.

We use 'Schrödinger cat' experiments with a single ion [19, 24] to analyse the forced motion and characterize light shifts. We then use the two-ion behaviour as a function of τ with no analysis pulse to diagnose the setup. We model the results by assuming each qubit decoheres independently at rate Γ. For the case of a $\mathcal{W}$ pulse only in the first gap, we then expect

$$P(\uparrow\uparrow) = A - \tfrac{1}{2}\mathrm{e}^{-\Gamma\tau - |\alpha(\tau)|^2/2}\cos(\Psi(\tau))\cos(\Delta_\mathrm{c}\tau) \qquad P(\uparrow\downarrow) + P(\downarrow\uparrow) = 1 - 2A \tag{4}$$

where $A = (1/4) + \mathrm{e}^{-2\Gamma\tau}(\cos(2\Delta_\mathrm{c}\tau) + \mathrm{e}^{-2|\alpha(\tau)|^2})/8$ and $\alpha(\tau)$, $\Psi(\tau)$ are the motional displacement and phase as described in [1]. Since the 866 nm laser is on throughout the sequence of coherent manipulations, there is negligible population in the $D_{3/2}$ level, and thus $P(\downarrow\downarrow) = 1 - P(\uparrow\uparrow) - P(\uparrow\downarrow) - P(\downarrow\uparrow)$. Data is shown in figure 2(a), fitted with floated parameters Γ, δ, Ω_f and $\Delta\phi$. We obtained $\Gamma = 5.4\,\text{ms}^{-1}$, $\delta/2\pi = 13\,\text{kHz}$, $\Omega_\mathrm{f}/2\pi = 23\,\text{kHz}$ and $\Delta\phi = 1.6$ from the fit; these values were consistent with our other information on δ, Ω_c and $\Delta\phi$. Note that $\Omega_\mathrm{f}/\delta \simeq \sqrt{3}$,

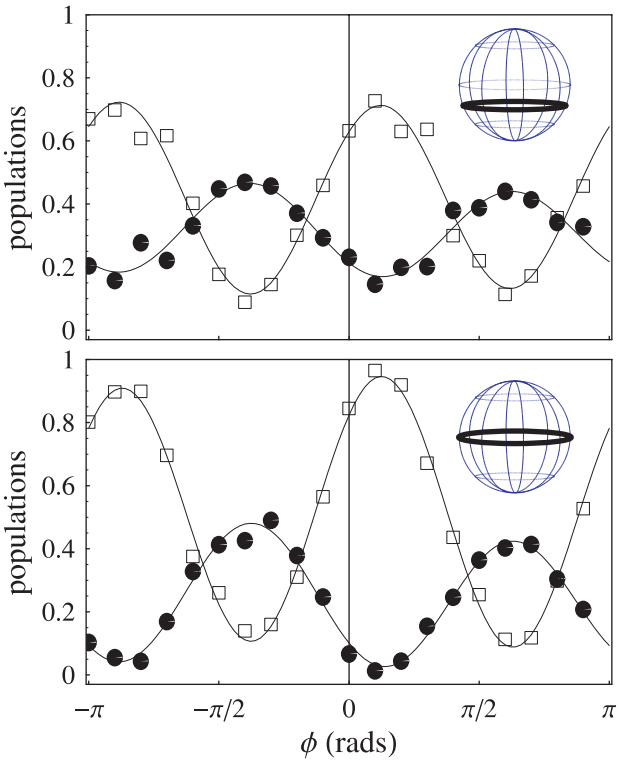

Figure 3. Tomography signals for spin state after the spin echo ($\mathcal{W}(44\,\mu s)$ in both gaps, $\delta/2\pi = 22.7$ kHz). The data points show $P_R(\uparrow\uparrow)$, $P_R(\uparrow\downarrow) + P_R(\downarrow\uparrow)$ (●, □) versus ϕ for $\theta = 0.66\pi$ (top panel) and $\theta = 0.54\pi$ (bottom panel), as deduced from 500 repeats of the experimental sequence. The lines are the fitted curves (1). θ values were deduced from carrier flopping signals, taking into account a 0.1 μs dead time in the AOM; ϕ is accurately known from the r.f. signal generators. Inset: locus of θ, ϕ values on the Bloch sphere.

so in this experiment $\Psi = 3\pi/2$. When we use the model and fitted values to infer ρ at $\tau = 2\pi/\delta$, we obtain fidelity $F = 0.7(1)$.

We next measured a lower bound more directly, $F \geqslant 2|C|$, by using an analysis pulse at $\theta = \pi/2$ to deduce the coherence $C = \rho_{\uparrow\uparrow,\downarrow\downarrow} = c_{11} - c_{22} + i(c_{12} + c_{21})$. This is obtained from the component at frequency 2 in the parity signal $1 - 2(P_R(\uparrow\downarrow) + P_R(\downarrow\uparrow))$ versus ϕ (data shown in figure 2(b)). We observed $F \geqslant 0.74(3)$. This result is more precise than the previous one because it does not rely on assumptions about the decoherence.

Finally, we performed tomography in another experiment where the $\mathcal{W}$ pulse was inserted in both gaps. This has the effect of cancelling the single-bit rotations $Z_k(\phi_1)$. Both pulses had the duration $\tau = 2\pi/\delta$, so the motion completes two loops in phase space, and the gate requires $\Psi = \pi/4$ for each loop. We set $\delta/2\pi = 22.7$ kHz and observed the signal with pulses of double length in order to adjust the laser intensity. We then used the carrier flopping rate to infer Ω_f, obtaining $2\pi \times 16.3(9)$ kHz, giving the consistency check $(\Omega_f/\delta)^2 = 0.52(5)$.

The data and fitted curves for the tomography are shown in figure 3, and the inferred (maximum likelihood) density matrix is shown in figure 4. Owing to the absence of single ion

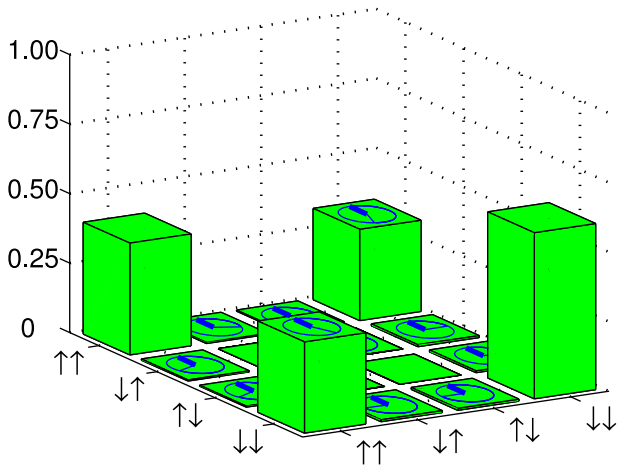

Figure 4. Density matrix obtained from tomography data shown in figure 3. The height of the bars indicates the absolute value of each density matrix element, and the clock faces indicate their phase. For this example, the density matrix is closest to the state (3) with $r = 1.15\pi$.

addressing in the rotations and the measurements, the tomography only gives partial information on the internal elements of ρ (i.e. away from the corners in figure 4). However, we find that there is negligible population in $|\uparrow\downarrow\rangle$ and $|\downarrow\uparrow\rangle$ and therefore for the state in question, the tomography is complete. The inferred ρ had fidelity $F = 0.83(2)$ and entanglement of formation [12] 0.54. The improvement is owing to better precision in pulse areas and a reduction in the total area by $\sqrt{2/3}$, which reduces decoherence by photon scattering.

We estimate that the primary source of infidelity is photon scattering (12%), with additional contributions from imbalance in light intensity at the ions, pulse area imprecision, and motional decoherence. Had we used a gate method which is more sensitive to the prepared motional state, such as [25], the thermal effect alone would contribute a further 6% infidelity through imprecise sideband pulses. We therefore obtained a useful improvement by using a temperature-insensitive method.

To conclude, we have implemented a two-qubit quantum logic gate between a pair of trapped ^{40}Ca ions with 83% fidelity. One of the notable features of our study is that the qubit is physically represented by a very good approximation to a strictly two-state system: leakage out of the computational Hilbert space is completely negligible after repumping by the 866 nm laser. We have also demonstrated the technical simplification of working with a single pair of laser beams for all coherent manipulations. This introduces an ac Stark shift whose effects are $O(\pi)$ and can be taken into account.

Acknowledgments

This study was supported by the EPSRC through QIP IRC, the Royal Society, the European Union through the FET project ‘QGATES’ and research training network ‘CONQUEST’, the National Security Agency (NSA) and Advanced Research and Development Activity (ARDA) (P-43513-PH-QCO-02107-1)

References

[1] Leibfried D *et al* 2003 Experimental demonstration of a robust, high-fidelity geometric two ion-qubit phase gate *Nature* **422** 412–5

[2] Milburn G J, Schneider S and James D F V 2000 Ion trap quantum computing with warm ions *Fortschr. Physik* **48** 801–10

[3] Sørensen A and Mølmer K 2000 Entanglement and quantum computation with ions in thermal motion *Phys. Rev.* A **62** 022311 (*Preprint* quant-ph/0002024)

[4] Wang X, Sørensen A and Mølmer K 2001 Multibit gates for quantum computing *Phys. Rev. Lett.* **86** 3907–10

[5] Sørensen A and Mølmer K 1999 Quantum computation with ions in thermal motion *Phys. Rev. Lett.* **82** 1971–4

[6] Turchette Q A, Wood C S, King B E, Myatt C J, Leibfried D, Itano W M, Monroe C and Wineland D J 1998 Deterministic entanglement of two trapped ions *Phys. Rev. Lett.* **81** 3631–4

[7] Haljan P C, Lee P J, Brickman K-A, Acton M, Deslauriers L and Monroe C 2005 Entanglement of trapped-ion clock states *Phys. Rev.* A **72** 062316

[8] Leibfried D *et al* 2005 Creation of a six-atom 'Schrodinger Cat' state *Nature* **438** 639–42

[9] Schmidt-Kaler F, Häffner H, Riebe M, Gulde S, Lancaster G P T, Deuschle T, Becher C, Roos C F, Eschner J and Blatt R 2003 Realization of the Cirac-Zoller controlled-NOT quantum gate *Nature* **422** 408–11

[10] Häffner H *et al* 2005 Scalable multiparticle entanglement of trapped ions *Nature* **438** 643

[11] Lo H-K, Popescu S and Spiller T (ed) 1998 *Introduction to Quantum Computation and Information* (Singapore: World Scientific)

[12] Nielsen M A and Chuang I L 2000 *Quantum Computation and Quantum Information* (Cambridge: Cambridge University Press)

[13] Lucas D M, Ramos A, Home J P, McDonnell M J, Nakayama S, Stacey J-P, Webster S C, Stacey D N and Steane A M 2004 Isotope-selective photo-ionisation for calcium ion trapping *Phys. Rev.* A **69** 012711

[14] Turchette Q A *et al* 2000 Heating of trapped ions from the quantum ground state *Phys. Rev.* A **61** 063418

[15] Deslauriers L, Haljan P C, Lee P J, Brickman K-A, Blinov B B, Madsen M J and Monroe C 2004 Zero-point cooling and low heating of trapped Cd ions *Phys. Rev.* A **70** 043408 (*Preprint* quant-ph/0404142)

[16] Wineland D J, Monroe C, Itano W M, Leibfried D, King B E and Meekhof D M 1998 Experimental issues in coherent quantum-state manipulation of trapped atomic ions *J. Res. Natl Instrum. Standard Technol.* **103** 259–328

[17] Kielpinski D, Monroe C and Wineland D 2002 Architecture for a large-scale ion-trap quantum computer *Nature* **417** 709–11

[18] Steane A 2004 How to build a 300 bit, 1 Gigaop quantum computer (*Preprint* quant-ph/0412165)

[19] McDonnell M J, Home J P, Lucas D M, Imreh G, Keitch B C, Szwer D J, Thomas N R, Webster S C, Stacey D N and Steane A M 2006 Long-lived mesoscopic entanglement outside the lamb-dicke regime (*Preprint* quant-ph/0605083)

[20] Paris M G A and Rehacek J (ed) 2004 *Quantum State Estimation* (Berlin: Springer)

[21] James D F V, Kwiat P G, Munro W J and White A G 2001 Measurement of qubits *Phys. Rev.* A **64** 052312

[22] McDonnell M, Stacey J-P, Webster S C, Home J P, Ramos A, Lucas D M, Stacey D N and Steane A M 2004 High-efficiency detection of a single quantum of angular momentum by suppression of optical pumping *Phys. Rev. Lett.* **93** 153601

[23] King B E, Wood C S, Myatt C J, Turchette Q A, Leibfried D, Itano W M, Monroe C and Wineland D J 1998 Cooling the collective motion of trapped ions to initialize a quantum register *Phys. Rev. Lett.* **81** 1525–8

[24] Monroe C, Meekhof D M, King B E and Wineland D J 1996 A 'Schrodinger Cat' superposition state of an atom *Science* 272 1131

[25] Cirac J I and Zoller P 1995 Quantum computations with cold trapped ions *Phys. Rev. Lett.* **74** 4091–4